

A Competitive Showcase of Quantum versus Classical Algorithms in Energy Coalition Formation

Naeimeh Mohseni,¹ Thomas Morstyn,² Corey O’Meara,¹ David Bucher,³ Jonas Nüßlein,⁴ and Giorgio Cortiana⁵

¹*E.ON Digital Technology GmbH, Tresckowstraße 5, Hannover, Germany,*

²*Department of Engineering Science, University of Oxford, UK*

³*Aqarios GmbH, Prinzregentenstraße 120, Munich, Germany*

⁴*Ludwig-Maximilians University Munich, Institute for Computer Science, Germany*

⁵*E.ON Digital Technology GmbH, Laatzenener Straße 1, Hannover, Germany,*

(Dated: May 21, 2024)

The formation of energy communities is pivotal for advancing decentralized and sustainable energy management. Within this context, Coalition Structure Generation (CSG) emerges as a promising framework. The complexity of CSG grows rapidly with the number of agents, making classical solvers impractical for even moderate sizes (number of agents > 30). Therefore, the development of advanced computational methods is essential. Motivated by this challenge, this study conducts a benchmark comparing classical solvers with quantum annealing on Dwave hardware and the Quantum Approximation Optimization Algorithm (QAOA) on both simulator and IBMQ hardware to address energy community formation. Our classical solvers include Tabu search, simulated annealing, and an exact classical solver. Our findings reveal that Dwave surpasses QAOA on hardware in terms of solution quality. Remarkably, QAOA demonstrates comparable runtime scaling with Dwave, albeit with a significantly larger prefactor. Notably, Dwave exhibits competitive performance compared to the classical solvers, achieving solutions of equal quality with more favorable runtime scaling.

I. INTRODUCTION

To explore the potential of quantum computing in optimization problems it is encouraging to benchmark quantum solvers against classical solvers in tackling problems that are sufficiently hard and exceed the capabilities of state-of-the-art classical solvers. This exploration becomes even more intriguing when problems get already hard in intermediate sizes where existing quantum hardware can be effectively leveraged. It is also crucial that the problem can be formulated compatible with existing quantum algorithms and hardware [1]. As we explain next, energy coalition formation applying the Coalition Structure Generation (CSG) game stands out as an exemplary candidate for such benchmarking, given its computational complexity and profound real-world significance within the industry. The formation of energy communities represents a significant step towards decentralized and sustainable energy management, offering opportunities for local empowerment, renewable energy adoption, and enhanced resilience in energy systems [2–4].

CSG provides a framework for understanding how agents, can form coalitions denoted by C_l (with l being the index of the coalition) to optimize their collective benefits [5–8]. A coalition within this context can be characterized by a characteristic function, typically denoted as $v(C_l)$, which assigns values to different coalitions. This specific type of cooperative game, defined by the characteristic function, is commonly referred to as a characteristic function game (CFG). The value function provides a measure of the cooperative advantage or payoff that the agents in the coalition can attain by working together, as opposed to operating independently [9, 10].

The task of creating coalition structures is highly challenging, especially given the presence of n agents, leading

to a staggering $O(n^n)$ possible partitions. Currently, the only algorithm capable of finding an optimal solution is the Dynamic Programming algorithm, achieving this in $O(3^n)$ time [11]. This approach is limited to systems consisting of a few tens of agents (i.e. $n < 25$). CFG can be transformed into an approximately equivalent game represented using the induced subgraph game (ISG) [12]. In this representation, nodes correspond to agents, and coalition values are reflected in pairwise interactions within a weighted graph, such that $v(C_l) = \sum_{(i,j) \in C_l} w_{ij}$ [9, 10]. The transformation of CFG to ISG allows the problem to be recast as quadratic unconstrained binary optimization (QUBO), enabling more computationally efficient approaches. Nonetheless, it is crucial to note that the problem remains NP-complete [9] such that leading classical solvers, such as DyCE [13] and CFSS [13] are limited in scalability and memory requirements. For instance, DyCE [13], which employs dynamic programming, is restricted to systems with around 25 agents due to its exponential memory complexity ($O(2^n)$) and lacks an anytime approach. CFSS can handle larger but shallow problems, yet still explores all possible solutions for complete graphs with a complexity of $O(n^n)$.

In this work, we propose a novel formulation of energy coalition formation that can be encapsulated within the framework of CFG. Our formulation specifically addresses the value that can be created by cooperative distributed energy resources utilization by net-metered energy coalitions, as well as the costs in terms of network constraint management that can occur if these coalitions are too dispersed. Additionally, we introduce a novel method for transforming the CFG framework into an ISG. We then apply the approximate method introduced in [14] to optimize energy community formation.

Under this approximation, the complexity of an exact

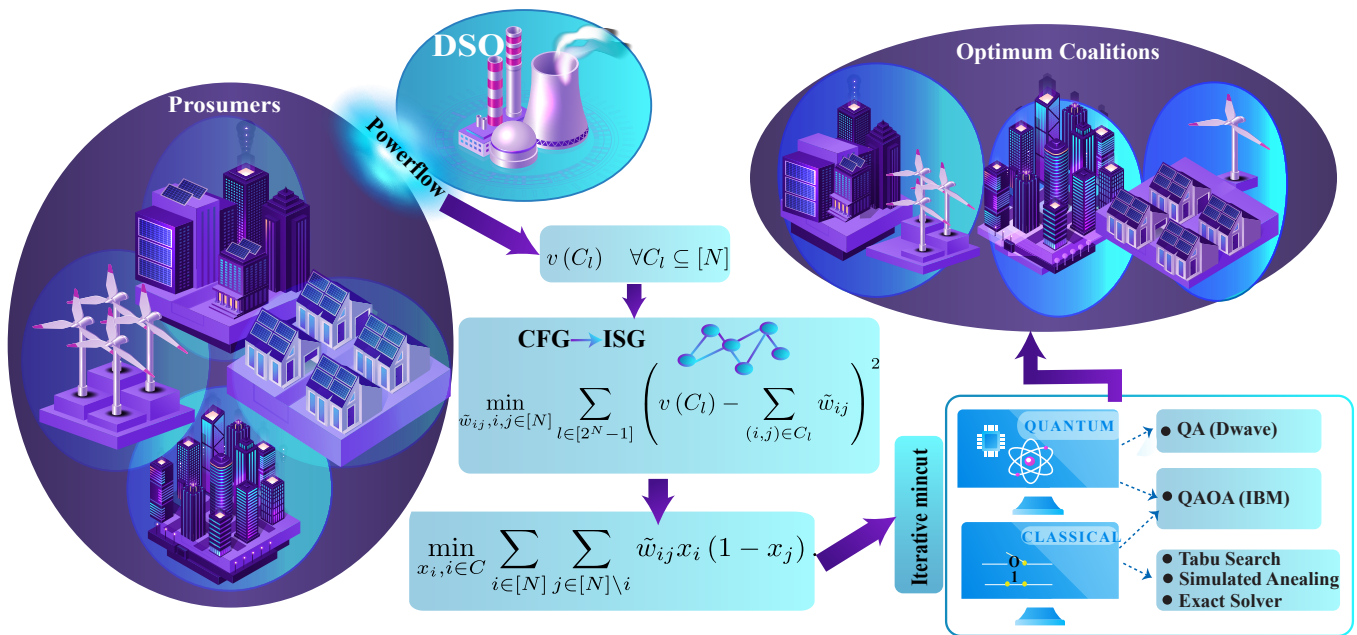


Figure 1. (a) Schematic representation of the workflow: The Distribution System Operator (DSO) strategically evaluates the potential of prosumer communities, aiming to minimize network management costs through optimized power flow analysis. The DSO’s decision-making involves partitioning prosumers into net-metered coalitions, treating it as a Characteristic Function Game (CFG) problem to optimize overall network efficiency. We transform the CFG formulation into the Induced Subgraph Game (ISG). An approximate solution to the ISG is found through iterative splitting coalitions to bipartitions until no value-increasing bipartitions remain. In the benchmarking phase, the efficiency of both quantum and classical solvers is assessed in the iterative splitting process.

solver remains $O(n^3)$ in time while numerical observation shows that an approximate classical solver can solve the problem in polynomial time. Our performance evaluation involves benchmarking an exact classical solver, Tabu search, simulated annealing, and QB-solve (an approximate classical solver developed by Dwave that employs the Tabu algorithm [15]) against quantum annealing on Dwave hardware, and the Quantum Approximation Optimization Algorithm (QAOA) on both simulators and IBMQ hardware.

Encouragingly, Dwave shows a competitive performance compared to our approximate classical solver. While it achieves solutions of equal quality to those found by the classical solvers, its runtime scales more favorably. This contrasts with many previous studies that demonstrate the poor performance of Dwave compared to state-of-the-art classical solvers on fully connected problems [16–19]. In previous works, the better performance of Dwave in comparison with classical solvers is mostly shown for the class of logical-planted problems that are constructed such that they promote the presence of tunneling barriers [20–22]. The competitive behavior that we observe in this work provides valuable insights into the potential advantages of quantum algorithms in the context of optimization problems.

We also show Dwave outperforms 1-round QAOA executed on hardware in terms of solution quality. Notably, QAOA demonstrates comparable runtime scaling with

Dwave albeit with a significantly larger prefactor. 1-round QAOA on the simulator represents a solution quality lower but still close to Dwave up to the system sizes we have been able to simulate.

Additionally, our experiments demonstrate that the solutions obtained through approximation on the ISG remain remarkably close to those derived from the original CFG formulation (up to system sizes that we have been able to check). This showcases the robustness and efficacy of our new introduced method in transferring CFG to ISG.

II. PROBLEM FORMULATION

Consider a distribution network with N prosumers (proactive consumers), each with some combination of inflexible loads, flexible loads, generation and/or storage. A standard arrangement for retail contracts is for each prosumer’s energy demand to be individually metered, with the net demand during each metering period t charged at an import price λ_t^b , and net supply rewarded at a lower export price $\lambda_t^s \leq \lambda_t^b$. An alternate arrangement is to enable groups of retail prosumers to form net-metered energy communities, where prosumers’ collective net demand is metered. This creates an overall incentive for community supply-demand balancing, and cooperative game theory can be used to calculate cost/revenue sharing which aligns

individual incentives with collective optimization. The energy management problem for each coalition with optimization horizon $[T]$, can be generically described by,

$$\begin{aligned} \min_{p_i, i \in [C_i]} \sum_{i \in [C_i]} c_i(p_i) \\ - \Delta_t \sum_{t \in [T]} \left(\lambda_t^b \left[\sum_{i \in [C_i]} p_{it} \right]^- + \lambda_t^s \left[\sum_{i \in [C_i]} p_{it} \right]^+ \right) \\ \text{s.t. } p_i \in \mathcal{P}_i, \forall i \in [C_i]. \end{aligned} \quad (1)$$

We label the N coalitions for which prosumers are metered individually C_i^0 . Here, $[p_{it}]^+ = \max\{0, p_{it}\}$ and $[p_{it}]^- = \min\{0, p_{it}\}$. p_{it} is the prosumer output power during time interval t and $p_i = (p_{i1}, \dots, p_{iT})$ is the vector of output powers over the time horizon. Δ_t is the duration of each time interval. Each prosumer has a cost function $c_i(p_i)$ associated with the usage of their flexible devices and a constraint set \mathcal{P}_i for their output power vector, which may be time-coupled. For the exact choice of $c_i(p_i)$ and constraint set \mathcal{P}_i , refer to Supplemental Material Sec. II.

The supply-demand balancing incentivized by community net metering is generally desirable for local groups of prosumers. However, when expanded to larger more dispersed groups, there is the potential that this will introduce distribution losses and the need for additional flexibility procurement to prevent network constraint violations. Consider the perspective of a distribution system operator (DSO), and assume it has the authority to allow or disallow the formation of net-metered energy communities. The DSO needs to be able to calculate the value in terms of reduced network management costs (which could be negative) of allowing a coalition of prosumers C_l to form a net-metered community. In general, network power flows and management costs will depend on the collective operation of all prosumers. To simplify the value calculation for coalition formation, we focus on the marginal value created assuming prosumers which are not in the coalition operate under individual metering. In this case, the value created can be approximated as,

$$\begin{aligned} v(C_l) &= \mathcal{O}^{opf*}(p_i^{\text{ind}*} \mid i \in [N]) - \mathcal{O}^{opf*}(p_i^{\text{net}*} \mid i \in [N]), \\ p_i^{\text{ind}*} &= p_i^* \text{ from (1) optimized for } C_i^0, \\ p_i^{\text{net}*} &= \begin{cases} p_i^* \text{ from (1) optimized for } C_l, & \text{if } i \in C_l, \\ p_i^* \text{ from (1) optimized for } C_i^0, & \text{otherwise} \end{cases} \end{aligned} \quad (2)$$

Here, $*$ indicates the solution to an optimization problem. $p_i^{\text{ind}*}$ ($p_i^{\text{net}*}$) represents the optimized power for the prosumer i under individual (net) metering. $[N] = 1, 2, \dots, N$ and \mathcal{O}^{opf*} is the objective function value for the following optimal power flow problem which the DSO can use to procure flexibility to manage losses and network constraints,

$$\begin{aligned} \min_{p_{kt}^\uparrow, p_{kt}^\downarrow, k \in [K], t \in [T]} \Delta_t \sum_{t \in [T]} \sum_{k \in [K]} \lambda_{kt}^\uparrow p_{kt}^\uparrow + \lambda_{kt}^\downarrow p_{kt}^\downarrow \\ \text{s.t. } \left\{ p_{kt}^\uparrow, p_{kt}^\downarrow \mid k \in [K] \right\} \in \mathcal{N}_t(p_{it}^* \mid i \in [N]), \forall t \in [T], \\ \left\{ p_{kt}^\uparrow, p_{kt}^\downarrow \mid t \in [T] \right\} \in \mathcal{P}_k^{\uparrow\downarrow}, \forall k \in [K]. \end{aligned} \quad (3)$$

$p_{kt}^\uparrow, p_{kt}^\downarrow$ are the costs of upward/downward flexibility at network node $k \in [K]$ during time interval $t \in [T]$, and $\lambda_{kt}^\uparrow, \lambda_{kt}^\downarrow$ are the associated prices. \mathcal{N}_t is the network constraint set for time interval t (e.g. nodal power balance, bus voltage limits, line power flow limits). Note that this constraint set will depend on the prosumer output powers from the retail market $p_{it}^*, i \in [N]$. $\mathcal{P}_k^{\uparrow\downarrow}$ is the constraint set for flexibility at network node k , which in general may be time-coupled. For more details on power flow optimization refer to Sec. II of supplemental Material.

The DNO decision problem is then to partition the prosumers into a set of net-metered coalitions with the goal of minimizing network management costs. This is formulated as a CFG problem, which can be solved using binary integer linear programming (BILP) [23],

$$\begin{aligned} \max_{x_l, l \in [2^N - 1]} \sum_{l \in [2^N - 1]} v(C_l) x_l, \\ \text{s.t. } \sum_{j \in [2^N - 1]} S_{il} x_l = 1, \forall i \in [N], \\ x_l \in \{0, 1\}, \forall l \in [2^N - 1]. \end{aligned} \quad (4)$$

Note that there are $2^N - 1$ potential sub-coalitions of prosumers. $S_{il} = 1$ if prosumer $i \in [N]$ belongs to coalition C_l (i.e. $i \in C_l$), and $S_{il} = 0$ otherwise. Binary decision variable $x_l = 1$ indicates that C_l is part of the selected partition, and the value function $v(C_l)$ gives the value of the coalition. This formulation is computationally intensive since the number of binary decision variables depends on the number of sub-coalitions, which increases exponentially with the number of prosumers (i.e. $2^N - 1$).

This CFG formulation can be transformed into ISGs, where the value of a coalition can be expressed as the sum of pair-wise ‘‘joint utilities’’ between prosumers $w_{ij} \in \mathbb{R}, i, j \in [N]$, i.e. $v^{\text{ISG}}(C_l) = \sum_{(i,j) \in C_l} w_{ij}$ with lower computational requirements. The value function nonlinearities mean this framework is not directly applicable to our CFG. However, we can make use of an ISG based on pairwise joint utilities \tilde{w}_{ij} which approximate our CFG. The following quadratic programming problem can be used to find pairwise weights that minimize the mean squared error between the value functions and an approximate ISG,

$$\min_{\tilde{w}_{ij}, i, j \in [N]} \sum_{l \in [2^N - 1]} \left(v(C_l) - \sum_{(i,j) \in C_l} \tilde{w}_{ij} \right)^2. \quad (5)$$

Starting with the grand coalition, an approximate solution to the ISG can be found by iteratively splitting

coalitions in two, until no value-increasing bipartitions are available [14]. For a given iteration, let $C \in [N]$, be one of the optimal bipartitions that was found. The optimal bipartitions of C at the next iteration can be found using the following quadratic unconstrained binary optimization (QUBO) with N binary decision variables,

$$\begin{aligned} \min_{x_i, i \in C} & \sum_{i \in [N]} \sum_{j \in [N] \setminus i} \tilde{w}_{ij} x_i (1 - x_j). \\ \text{s.t. } & x_i \in \{0, 1\}, \forall i \in [N]. \end{aligned} \quad (6)$$

The schematic representation of the workflow is shown in Fig. 1.

III. RESULTS

Before presenting the benchmarking results, it is essential first to elucidate the structure and complexity of our problem instances.

Problem Structure: Our analysis reveals that the graphs resulting from the mapping of CFG to ISG are almost fully connected across all system sizes, with connectivity levels exceeding 95 percent. Moreover, the weight distribution includes both positive and negative values forming a Gaussian distribution centered closely around zero. The light blue histogram depicted in Fig. 2 lower right panel illustrates the weight distribution for the case of 18 prosumers averaging over 20 instances (different instances of the problem correspond to different initial power configurations for prosumers at the outset and varying export and import prices). This scenario, characterized by a fully connected graph featuring a mixture of positive and negative weights, represents a particularly challenging case [24]. For further insights, refer [24], where they discuss the boundary between polynomially-solvable Max Cut and NP-Hard Max Cut instances when they are classified only on the basis of the sign pattern of the objective function coefficients.

Benchmark: Now, we elaborate on the outcome of an extensive performance evaluation, benchmarking an exact classical solver and QB-solve [15] against quantum annealing on Dwave hardware (Dwave Advantage 4.1), and QAOA on both the simulator and IBMQ hardware (IBM-Osaka). QB-solve is a decomposing solver that uses the Tabu algorithm [25, 26] for solving sub-problems. In addition to these solvers, we also include results obtained using a random sampler which is beneficial as it provides a baseline comparison to gauge the efficacy of the solvers. For a detailed overview of all the solvers utilized in our benchmarking process refer to Supplemental Material Sec. I.

We benchmark the performances in terms of solution quality and running time (Fig. 2). The run time for all solvers encompasses any pre or post-processing time. The results for each number of prosumers showcase averages across 20 realizations except for IBM hardware and random solver with 2^{12} shots where results are shown for a single problem instance per data point.

Solution Quality: In Fig. 2 (a) and (b), we present the solution quality for both the transferred formulation, namely ISG, and the original formulation, CFG, respectively. For ISG, the solution quality, for up to 30 prosumers, is defined as the ratio of the value of the optimal coalition obtained from any solver on our ISG formulation to the value determined by the exact solver on our ISG formulation. In scenarios involving more than 30 prosumers, where the exact solution on ISG is unknown, the baseline is established by the optimal coalition obtained through QB-solve. Panel (b) shows the solution quality for the original CFG problem, where the solution quality is defined as the ratio of the optimal coalition value obtained from any solver on ISG to the baseline value determined by improved dynamic programming (IDP) on CFG. Further details about IDP can be found in [11]. Note that IDP is the only existing algorithm capable of finding an optimal solution for the CFG. Since IDP requires a considerable amount of time, typically takes several hours for 20 prosumers, thus limiting our ability to find solution quality for larger sizes.

Dwave and QB-solve exhibit comparable solution quality on both ISG and CFG. It is very encouraging to see that solutions obtained through approximation on the ISG remain remarkably close to those derived from the original CFG formulation. This confirms the efficacy of the mapping that we introduced in Eq. 5.

The 1-round QAOA executed on the simulator reveals a solution quality slightly lower, yet still close to that of Dwave and QB-solve. Enhancing the solution quality is still feasible by increasing the number of rounds. However, when executed on IBM hardware, the solution quality experiences a drastic decrease with system size. At times, it performs marginally better than a random sampler with the same number of shots, while at other times, it closely resembles the performance of a random solver. It is important to note that drawing a conclusive assessment would ideally involve averaging over a significant number of samples. However, such an analysis demands considerable resources, which we were unable to allocate.

Several factors contribute to the suboptimal performance of QAOA on hardware platforms, leaving room for improvement. Firstly, the original QAOA ansatz is inefficient and hardware-unfriendly for dense models. Recent studies have introduced new modified ansätze for QAOA that are more hardware-friendly [27, 28]. However, the effectiveness of these ansätze for fully connected models has yet to be thoroughly investigated. Secondly, additional efforts are necessary to transpile the circuit into a more hardware-friendly form [29, 30]. As illustrated in Fig. 2 (d), the circuit depth increases quadratically with the number of qubits. The existing transpiling methods may improve the efficiency of QAOA but they still highlight further obstacles to improve to make QAOA competitive [29, 30]. Moreover, here we just applied error mitigation in the readout, implementing additional mitigation schemes is required for QAOA [31].

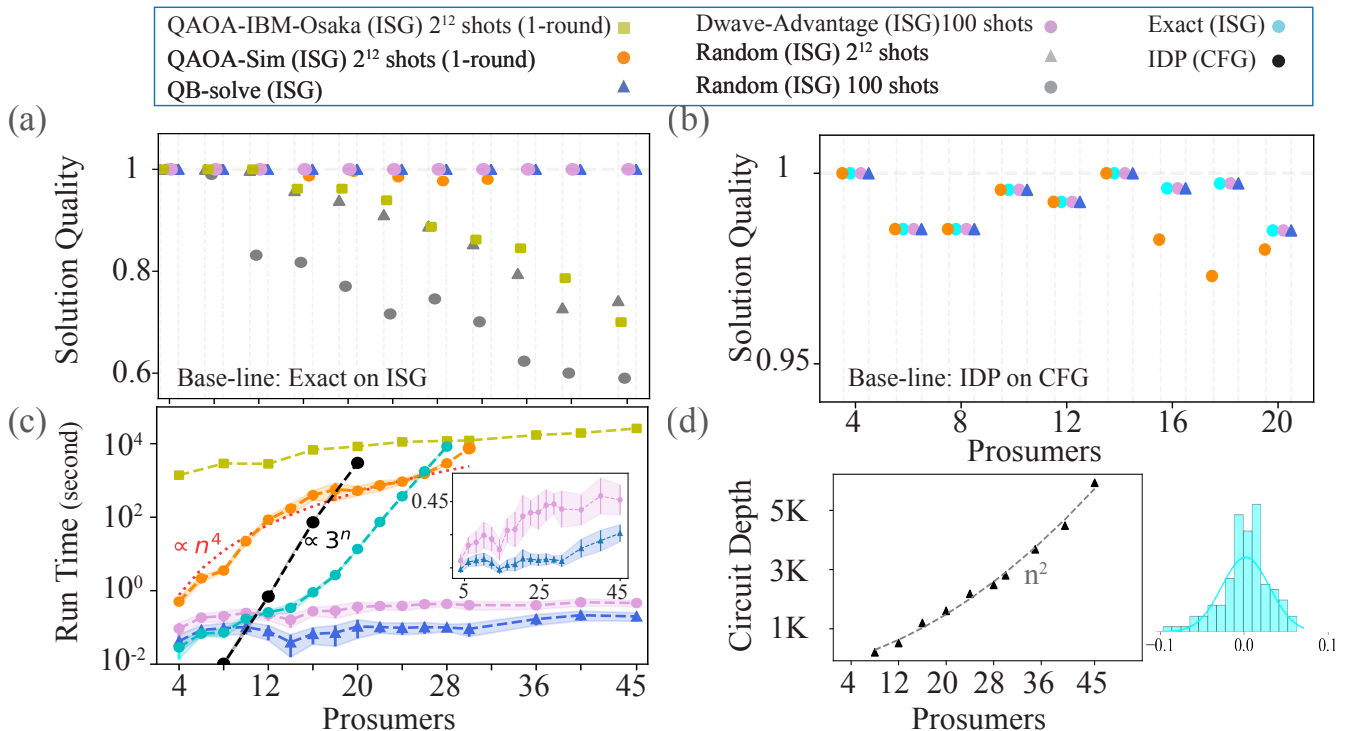


Figure 2. Benchmarking classical solvers against quantum solvers in energy coalition formation: (a) Solution quality of different solvers on ISG where the baseline is w.r.t. the solution determined with the exact solver on ISG. (b) The solution quality of different solvers on ISG w.r.t. the solution determined with IDP on the original CFG formulation. (c) Run time of different solvers on ISG as well as run time of improved dynamical programming (IDP) on CFG. Dwave and QB-solve curves are shown again in the inset to provide a closer examination of scaling. (d) QAOA circuit depth on quantum hardware for different numbers of prosumers (number of qubits). Results for each number of prosumers showcase averages across 20 realizations except for IBM hardware and random solver with 2^{12} where results are shown for a single problem instance per data point. The light blue histogram on the lower right shows the weight distribution after transferring CFG to ISG.

Run Time: Fig. 2 (c), shows the run time of different solvers. For a closer examination of scaling, we have included Dwave and QB-solve run time separately again in the inset. Dwave and QB-solve demonstrate competitive runtime however up to 45 prosumers it is hard to see a clear scaling. The exact classical solver on ISG and CFG, due to their computational complexity, experience a noticeable increase in runtime that become impractical beyond 30 prosumers. The runtime of QAOA on the simulator exhibits polynomial scaling, though sub-optimal. Interestingly, the scaling behavior of QAOA on Hardware is close to Dwave and QB-solve, albeit with a significantly larger prefactor. This can be attributed to iteratively updating variational parameters and running the algorithm on hardware for each parameter update. Initializing variational parameters based on existing heuristic schemes [32, 33] or learning them via machine learning techniques [34, 35] could significantly reduce this prefactor.

Randomly generated problems: To enhance the robustness of our findings and gain deeper insights into the performance scalability of D-Wave, we validate our results on larger-scale random problems by generating our

problem instances randomly. Solving power flow equations for more than a few tens of prosumers demands substantial computational resources, and for the scope of this work, random generation suffices. For smaller numbers of prosumers, the distribution of generated problems, after transforming from CFG to ISG, follows a Gaussian distribution centered around zero with a width of 0.2 across all prosumer sizes. Therefore, for larger sizes, we generate our problem instances using the same Gaussian distribution but intentionally vary the width to 2. This deliberate variation allows us to investigate the correlation between solvers' performance and distribution characteristics, which may align with different choices of constraints and parameters in the problem formulation

The outcome of this investigation is presented in Fig. 3. For a more comprehensive benchmark, we additionally employ two other classical solvers: simulated annealing and Tabu search. Given that the exact solution is unknown for large system sizes, we assess the quality of solutions by calculating the sum of values from the optimum coalitions, divided by the number of prosumers. A higher value signifies a superior solution. Dwave consistently demonstrates

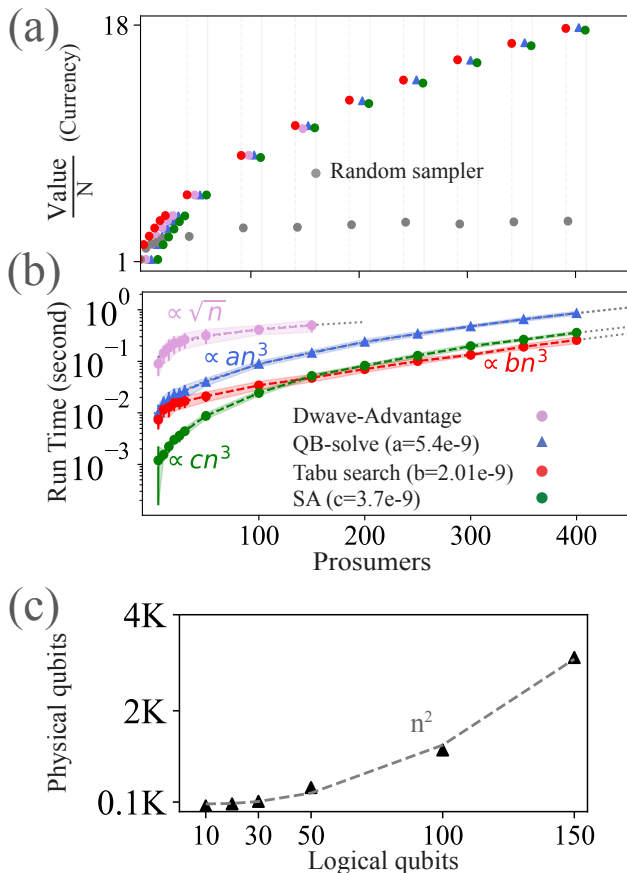


Figure 3. Benchmarking classical solvers against Dwave in energy coalition formation for randomly generated problems (sourced from the same distribution as the real use case problems namely a Gaussian distribution with a width of 2). (a) The solution quality (Average value per prosumer) versus the number of prosumers. (b) Run time versus number of prosumers. Results for each number of prosumers showcase averages across 20 realizations. (c) The number of physical qubits versus logical qubits (number of prosumers) on Dwave hardware for the first split of the grand coalition into two partitions.

performance in line with the results depicted in Fig. 2 and competes effectively with the classical solvers. Up to the scale implemented on the hardware, Dwave demonstrates a more favorable runtime scaling as a function of problem size, as depicted in Fig. 3(b). The runtime of QB-solve, Tabu search, and simulated annealing scales cubically with varying prefactors, with Tabu search exhibiting the lowest prefactor. In contrast, Dwave’s runtime scales as \sqrt{n} with n the number of prosumers. At the same time, all solvers produce solutions of almost equal values, as shown in Fig. 3(a).

When using the D-Wave quantum computer to solve a problem, the connectivity of the logical qubits in the problem must be mapped onto the hardware’s connectivity graph, which, for Advantage quantum processing units, is based on the Pegasus graph topology. This mapping

process typically necessitates additional qubits, known as physical qubits, beyond those required by the original problem. Figure 3 (c) illustrates the scaling of physical qubits with the number of logical qubits (prosumers).

IV. CONCLUSION AND OUTLOOK

The formation of energy communities signifies a pivotal shift towards decentralized and sustainable energy management. We employ the characteristic function game, offering a framework to comprehend how prosumers can unite in coalitions to maximize their collective advantages. A pivotal aspect of our approach is the exploration of optimal coalition compositions, balancing the benefits derived from increased resources for cooperative optimization against the network constraints and losses incurred when coalitions are dispersed. We conduct a benchmark comparing classical solvers with quantum solvers in this problem domain. Our findings showcase that the Dwave machine outperforms QAOA across hardware in terms of solution quality. However, it is important to note that the implementation of QAOA lacks intensive optimization in hardware resources and error mitigation schemes and there is still significant potential for further improvement in the performance of QAOA. Interestingly, QAOA demonstrates comparable runtime scaling with Dwave, albeit with a notably larger prefactor. Dwave exhibits competitive performance compared to our approximate classical solvers. While it achieves solutions of equal quality to those found by Tabu search and SA, its runtime is notably more favorable. This parity in performance highlights the promising potential of quantum algorithms in tackling optimization problems. The competitive performance shown by Dwave on our fully connected problems stands in contrast to its poor performance in previous studies [16–19].

It is essential to acknowledge that classical solvers have benefited from decades of development, while quantum solvers are still in their early stages of evolution. Therefore, the observed competitive performance highlights the evolving potential of quantum computing in optimization problems.

ACKNOWLEDGMENTS

N.M. would like to thank Supreeth Mysore, Ivan Angelov, Stefan Wörner, and Gabriele Agliardi for fruitful discussions. T. M. acknowledges the UK Engineering and Physical Sciences Research Council (EPSRC) (grant reference number EP/Y004418/1).

This work was supported by the German Federal Ministry of Education and Research under the funding program “Förderprogramm Quantentechnologien – von den Grundlagen zum Markt” (funding program quantum technologies — from basic research to market), project Q-Grid, 13N16177.

Supplemental Material

In this Supplemental Material, we provide a brief review of the algorithms that we applied in this work. We also provide further details on the formulation of our energy community formation problem.

I. ALGORITHMS

In this section, we provide a concise overview of the operational mechanisms of classical and quantum algorithms employed in this study.

A. Quantum Algorithms

1. Quantum Annealing

Quantum annealing (QA) is a heuristic algorithm based on the quantum adiabatic theorem [36, 37]. In this algorithm, the system is initially prepared in the ground state of a Hamiltonian H_0 where its ground state is known. A common choice for this initial Hamiltonian is $H_0 = -\sum_{i=1}^N \sigma_i^x$, where N denotes the number of qubits, and the ground state is the uniform superposition of all possible configurations $|+\rangle^{\otimes N}$ with $|+\rangle = (|0\rangle + |1\rangle)/\sqrt{2}$. The Hamiltonian is gradually reweighted to the desired problem Hamiltonian H_C according to

$$H = (1 - \lambda(t))H_0 + \lambda(t)H_C, \quad (\text{S1})$$

where $\lambda(t) \in [0, 1]$ is the annealing schedule. The annealing process can be viewed as H_0 introducing quantum fluctuations originating from the non-commutability of H_C and H_0 . These fluctuations are gradually reduced to reach the low-energy configuration of the classical energy function H_C . Based on the quantum adiabatic theorem, if one performs the sweep sufficiently slowly, the system remains in its instantaneous ground state throughout the evolution (Fig. S1 (a)) [36, 37]. H_C in our formulation is Eq. (6) at each min cut iteration. The number of qubits is then the number of prosumers. The use of quantum fluctuations in QA has been hypothesized as a potential resource for a speedup over classical methods. Quantum tunneling allows the system to pass through energy barriers that have a higher energy than available in the state [20].

2. Quantum Approximate Optimization Algorithm

QAOA can be seen as a trotterized version of QA. In QAOA [38], the system is initially prepared in $|+\rangle^{\otimes N}$. Then, unitary operators $U(\gamma_p, H_C) = e^{-i\gamma_p H_C}$ (corresponding to the cost Hamiltonian H_C) and $U(\beta_p) = e^{-i\beta_p H_0}$ (correspond to the mixer Hamiltonian $H_0 = \sum_{i=1}^N \sigma_i^x$) are applied, alternatively, generating the fol-

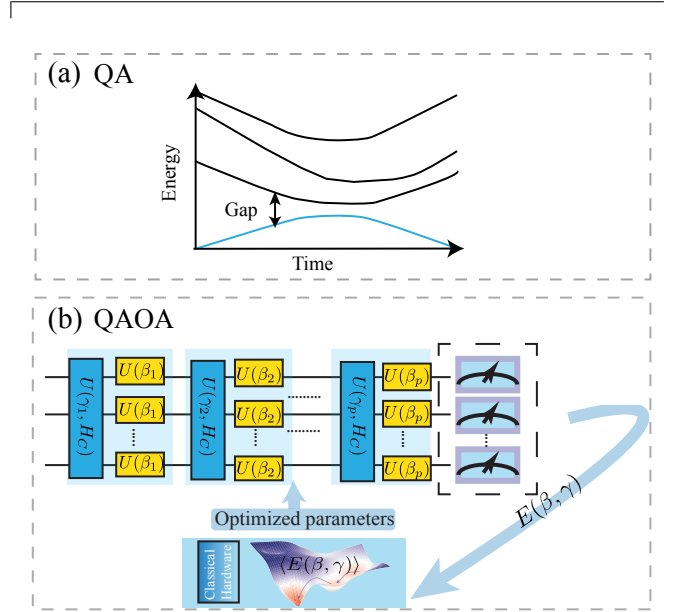


Figure S1. Schematic representation of QA and QAOA.

lowing variational quantum state:

$$|\psi(\boldsymbol{\beta}, \boldsymbol{\gamma})\rangle = e^{-i\beta_p H_0} e^{-i\gamma_p H_C} \dots e^{-i\beta_1 H_0} e^{-i\gamma_1 H_C} |+\rangle^{\otimes N}, \quad (\text{S2})$$

where $\boldsymbol{\gamma} = (\gamma_1, \gamma_2, \dots, \gamma_p) \in [0, 2\pi]^p$ and $\boldsymbol{\beta} = (\beta_1, \beta_2, \dots, \beta_p) \in [0, \pi]^p$ are $2p$ variational parameters and p determines the QAOA depth (number of rounds). Then, a classical optimizer is applied to find the optimal $(\boldsymbol{\beta}, \boldsymbol{\gamma})$ that optimizes the energy expectation $E(\boldsymbol{\beta}, \boldsymbol{\gamma}) = \langle \psi(\boldsymbol{\beta}, \boldsymbol{\gamma}) | H_C | \psi(\boldsymbol{\beta}, \boldsymbol{\gamma}) \rangle$ by updating the variational parameters iteratively (In this study, we applied Cobyla as our classical Optimizer). The parameterized quantum circuit transfers the initial state to the ground state of the target problem Hamiltonian. Fig. S1 (b) shows the schematic representation of the algorithm.

B. Classical Algorithms

1. Tabu Search

Tabu search is a metaheuristic optimization algorithm [25, 26]. Inspired by the concept of “taboo” this method strategically avoids revisiting previously explored solutions, preventing the algorithm from becoming trapped in local optima. By employing a short-term memory mechanism, Tabu search navigates the solution space by iteratively exploring neighboring solutions while adhering to tabu criteria that guide the search toward promising

regions. Its balance between exploration and exploitation makes it a versatile and effective tool for addressing optimization challenges.

2. *QB-solve*

The QB-solve tackles the challenge of finding the minimum value of large quadratic unconstrained binary optimization (QUBO) problems by breaking them into manageable pieces. It decomposes the global problem into smaller sub-problems by fixing certain bits and optimizing for those with the largest energy impact. This decomposition strategy allows QBsolve to focus on specific regions of the solution space where improvements are likely to have the greatest impact. Each piece is then solved using a specified solver, where here we use the Tabu algorithm [15].

3. *Simulated annealing*

Simulated annealing [39], inspired by the physical process of annealing in metallurgy, stands as a heuristic tool in the realm of optimization algorithms. At its core, simulated annealing begins with an initial solution and iteratively explores nearby solutions, accepting those that improve upon the current state while occasionally allowing for worse solutions to be accepted probabilistically. This acceptance of inferior solutions is controlled by a temperature parameter, which acts as a guiding force: at higher temperatures, the algorithm is more likely to accept poorer solutions, akin to the exploratory phase of the annealing process. However, as the algorithm progresses, this temperature parameter gradually decreases, reducing the likelihood of accepting suboptimal solutions and guiding the search towards convergence.

4. *Random Sampler*

In this work, we apply the random sampler in the dimod package ¹. The random sampler generates a specified number of random configurations (number of shots specified by the user), which represent assignments of values to variables within the problem space defined by the binary quadratic model (BQM). Each configuration serves as a potential solution to the optimization problem. Subsequently, the sampler calculates the objective value for each generated configuration. Among these configurations, the sampler identifies and selects the one with the lowest objective value as the solution.

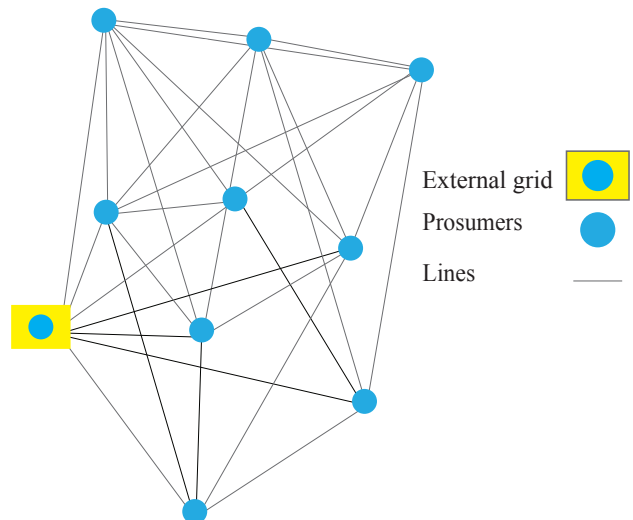


Figure S2. Schematic representation of the network with 9 prosumers and one external grid.

II. TECHNICAL DETAILS ON PROBLEM FORMULATION

The cost function $c_i(p_i)$ in Eq (1) can be chosen to be either linear or nonlinear, depending on the specific characteristics of prosumers and the energy system. We opt for a linear cost function, $c_i(p_i) = a_i p_i + b_i$, with $a_i = 1$ and $b_i = 0$ for simplicity. This choice may not fully capture all nuances of the prosumer’s behavior and system dynamics. However, it suffices for our purpose.

We establish distinct constraints for agents based on their roles as prosumers, pure consumers, or pure producers at each time. We designate 90 percent of all agents as prosumers, denoting individuals capable of both producing and consuming energy. The remaining 10 percent are randomly assigned as either pure consumers or pure producers. For all prosumers across all time steps, constraints on power levels (p_{it}) in Eq. (1) are established relative to their initial power levels (p_{it}^{initial}). This allows for fluctuations within a defined flexibility ϵ , set to 0.5 here. The initial power of prosumers are sourced from a simulation package that selects a specific location (e.g. Munich) and gathers information, including the number of residential, commercial, and industrial buildings. This data, leveraging standard load profiles and incorporating factors such as the number of households, shops, and industries, as well as their energy usage patterns, enables the estimation of power over time.

For agents that are prosumers, the power is bounded as follows

- When ($p_{it}^{\text{initial}} > 0$):

$$-p_{it}^{\text{initial}}(1 + \epsilon) \leq p_{i,t} \leq p_{it}^{\text{initial}}(1 + \epsilon)$$

¹ <https://docs.ocean.dwavesys.com/en/stable/docsdimod/>

- When ($p_{it}^{\text{initial}} < 0$):

$$p_{it}^{\text{initial}}(1 + \epsilon) \leq p_{i,t} \leq -p_{it}^{\text{initial}}(1 + \epsilon)$$

For agents that are pure producers ($p_{it}^{\text{initial}} > 0$) the power is bounded as:

$$0 \leq p_{i,t} \leq p_{it}^{\text{initial}}(1 + \epsilon)$$

For agents that are pure consumers ($p_{it}^{\text{initial}} < 0$) the power is bounded as:

$$p_{it}^{\text{initial}}(1 + \epsilon) \leq p_{i,t} \leq 0$$

The import and export price schedules are established by analyzing the CO_2 intensity derived from real-world

data collected in Munich². In our study, we utilize an external grid, which functions as a Distribution System Operator (DSO). The external grid acts as a point of connection for exchanging energy to/from prosumers. A schematic representation of our network is shown in Fig. S2. We consider four time steps. Each time step represents a 15-minute interval, capturing a comprehensive one-hour time window.

For power flow optimization, we use Panda Power, a Python-based library for power systems[40]. We employ the DC optimal power flow (DCPF) method within the Panda Power framework to optimize power flow across the network. Within Panda Power, we model the cost behavior using piece-wise linear (PWL) cost functions. These functions provide a realistic representation of generation costs by capturing nonlinear cost variations.

-
- [1] Amira Abbas, Andris Ambainis, Brandon Augustino, Andreas Bärtschi, Harry Buhrman, Carleton Coffrin, Giorgio Cortiana, Vedran Dunjko, Daniel J Egger, Bruce G Elmegreen, *et al.*, “Quantum optimization: Potential, challenges, and the path forward,” arXiv preprint arXiv:2312.02279 (2023).
 - [2] Wayes Tushar, Tapan Kumar Saha, Chau Yuen, M Imran Azim, Thomas Morstyn, H Vincent Poor, Dustin Niyato, and Richard Bean, “A coalition formation game framework for peer-to-peer energy trading,” *Applied Energy* **261**, 114436 (2020).
 - [3] Xi Luo and Yanfeng Liu, “A multiple-coalition-based energy trading scheme of hierarchical integrated energy systems,” *Sustainable Cities and Society* **64**, 102518 (2021).
 - [4] Jonas Blenninger, David Bucher, Giorgio Cortiana, Kumar Ghosh, Naeimeh Mohseni, Jonas Nüßlein, Corey O’Meara, Daniel Porawski, and Benedikt Wimmer, “Quantum optimization for the future energy grid: Summary and quantum utility prospects,” arXiv preprint arXiv:2403.17495 (2024).
 - [5] Filipe Bandejas, Álvaro Gomes, Mário Gomes, and Paulo Coelho, “Application and challenges of coalitional game theory in power systems for sustainable energy trading communities,” *Energies* **16**, 8115 (2023).
 - [6] Milad Moafi, Reza Rouhi Ardeshiri, Manthila Wijesooriya Mudiyansele, Mousa Marzband, Abdullah Abusorrah, Muhyaddin Rawa, and Josep M Guerrero, “Optimal coalition formation and maximum profit allocation for distributed energy resources in smart grids based on cooperative game theory,” *International Journal of Electrical Power & Energy Systems* **144**, 108492 (2023).
 - [7] Liyang Han, Thomas Morstyn, and Malcolm McCulloch, “Incentivizing prosumer coalitions with energy management using cooperative game theory,” *IEEE Transactions on Power Systems* **34**, 303–313 (2018).
 - [8] Talal Rahwan, Tomasz P Michalak, Michael Wooldridge, and Nicholas R Jennings, “Coalition structure generation: A survey,” *Artificial Intelligence* **229**, 139–174 (2015).
 - [9] Yoram Bachrach, Pushmeet Kohli, Vladimir Kolmogorov, and Morteza Zadimoghaddam, “Optimal coalition structure generation in cooperative graph games,” in *Proceedings of the AAAI Conference on Artificial Intelligence*, Vol. 27 (2013) pp. 81–87.
 - [10] Xiaotie Deng and Christos H Papadimitriou, “On the complexity of cooperative solution concepts,” *Mathematics of operations research* **19**, 257–266 (1994).
 - [11] Talal Rahwan and Nicholas R Jennings, “An improved dynamic programming algorithm for coalition structure generation,” (2008).
 - [12] Filippo Bistaffa, Georgios Chalkiadakis, and Alessandro Farinelli, “Efficient coalition structure generation via approximately equivalent induced subgraph games,” *IEEE Transactions on Cybernetics* **52**, 5548–5558 (2022).
 - [13] Filippo Bistaffa, Alessandro Farinelli, Jesús Cerquides, Juan Antonio Rodríguez-Aguilar, and Sarvapali D Ramchurn, “Anytime coalition structure generation on synergy graphs,” (2014).
 - [14] Supreeth Mysore Venkatesh, Antonio Macaluso, and Matthias Klusch, “Quacs: Variational quantum algorithm for coalition structure generation in induced subgraph games,” arXiv preprint arXiv:2304.07218 (2023).
 - [15] Michael Booth, Steven P Reinhardt, and Aidan Roy, “Partitioning optimization problems for hybrid classical, quantum execution. Technical Report , 01–09 (2017).
 - [16] Naeimeh Mohseni, Peter L McMahon, and Tim Byrnes, “Ising machines as hardware solvers of combinatorial optimization problems,” *Nature Reviews Physics* **4**, 363–379 (2022).
 - [17] Rhonda Au-Yeung, Nicholas Chancellor, and Pascal Halfmann, “Np-hard but no longer hard to solve? using quantum computing to tackle optimization problems,” *Frontiers in Quantum Science and Technology* **2**, 1128576 (2023).
 - [18] Daniel Vert, Renaud Sirdey, and Stéphane Louise, “Benchmarking quantum annealing against “hard” instances of the bipartite matching problem,” *SN Computer Science*

² <https://www.bayernwerk.de/de/fuer-zuhause/oekoheld.html>

- 2**, 1–12 (2021).
- [19] Costantino Carugno, Maurizio Ferrari Dacrema, and Paolo Cremonesi, “Evaluating the job shop scheduling problem on a d-wave quantum annealer,” *Scientific Reports* **12**, 6539 (2022).
- [20] Vasil S Denchev, Sergio Boixo, Sergei V Isakov, Nan Ding, Ryan Babbush, Vadim Smelyanskiy, John Martinis, and Hartmut Neven, “What is the computational value of finite-range tunneling?” *Physical Review X* **6**, 031015 (2016).
- [21] Salvatore Mandra and Helmut G Katzgraber, “A deceptive step towards quantum speedup detection,” *Quantum Science and Technology* **3**, 04LT01 (2018).
- [22] Tameem Albash and Daniel A. Lidar, “Demonstration of a scaling advantage for a quantum annealer over simulated annealing,” *Phys. Rev. X* **8**, 031016 (2018).
- [23] Supreeth Mysore Venkatesh, Antonio Macaluso, and Matthias Klusch, “Gcs-q: Quantum graph coalition structure generation,” in *International Conference on Computational Science* (Springer, 2023) pp. 138–152.
- [24] S Thomas McCormick, M Rammohan Rao, and Giovanni Rinaldi, “Easy and difficult objective functions for max cut,” *Mathematical programming* **94**, 459–466 (2003).
- [25] Gintaras Palubeckis, “Multistart tabu search strategies for the unconstrained binary quadratic optimization problem,” *Annals of Operations Research* **131**, 259–282 (2004).
- [26] Fred Glover, “Future paths for integer programming and links to artificial intelligence,” *Computers & operations research* **13**, 533–549 (1986).
- [27] David Amaro, Carlo Modica, Matthias Rosenkranz, Matia Fiorentini, Marcello Benedetti, and Michael Lubasch, “Filtering variational quantum algorithms for combinatorial optimization,” *Quantum Science and Technology* **7**, 015021 (2022).
- [28] Yunlong Yu, Chenfeng Cao, Carter Dewey, Xiang-Bin Wang, Nic Shannon, and Robert Joynt, “Quantum approximate optimization algorithm with adaptive bias fields,” *Phys. Rev. Res.* **4**, 023249 (2022).
- [29] Atsushi Matsuo, Shigeru Yamashita, and Daniel J Egger, “A sat approach to the initial mapping problem in swap gate insertion for commuting gates,” *IEICE Transactions on Fundamentals of Electronics, Communications and Computer Sciences* **106**, 1424–1431 (2023).
- [30] Johannes Weidenfeller, Lucia C Valor, Julien Gacon, Caroline Tornow, Luciano Bello, Stefan Woerner, and Daniel J Egger, “Scaling of the quantum approximate optimization algorithm on superconducting qubit based hardware,” *Quantum* **6**, 870 (2022).
- [31] Stefan H Sack and Daniel J Egger, “Large-scale quantum approximate optimization on nonplanar graphs with machine learning noise mitigation,” *Physical Review Research* **6**, 013223 (2024).
- [32] Leo Zhou, Sheng-Tao Wang, Soonwon Choi, Hannes Pichler, and Mikhail D. Lukin, “Quantum approximate optimization algorithm: Performance, mechanism, and implementation on near-term devices,” *Phys. Rev. X* **10**, 021067 (2020).
- [33] Vishwanathan Akshay, Daniil Rabinovich, Ernesto Campos, and Jacob Biamonte, “Parameter concentrations in quantum approximate optimization,” *Physical Review A* **104**, L010401 (2021).
- [34] JA Montanez-Barrera, Dennis Willsch, and Kristel Michielsen, “Transfer learning of optimal qaoa parameters in combinatorial optimization,” *arXiv preprint arXiv:2402.05549* (2024).
- [35] Naeimeh Mohseni, Junheng Shi, Tim Byrnes, and Michael Hartmann, “Deep learning of many-body observables and quantum information scrambling,” *arXiv preprint arXiv:2302.04621* (2023).
- [36] Edward Farhi, Jeffrey Goldstone, Sam Gutmann, and Michael Sipser, “Quantum computation by adiabatic evolution,” *arXiv preprint quant-ph/0001106* (2000).
- [37] Tameem Albash and Daniel A. Lidar, “Adiabatic quantum computation,” *Rev. Mod. Phys.* **90**, 015002 (2018).
- [38] Edward Farhi, Jeffrey Goldstone, and Sam Gutmann, “A quantum approximate optimization algorithm,” *arXiv preprint arXiv:1411.4028* (2014).
- [39] Scott Kirkpatrick, C Daniel Gelatt Jr, and Mario P Vecchi, “Optimization by simulated annealing,” *science* **220**, 671–680 (1983).
- [40] Leon Thurner, Alexander Scheidler, Florian Schäfer, Jan-Hendrik Menke, Julian Dollichon, Friederike Meier, Steffen Meinecke, and Martin Braun, “pandapower—an open-source python tool for convenient modeling, analysis, and optimization of electric power systems,” *IEEE Transactions on Power Systems* **33**, 6510–6521 (2018).